Interactions of Cyclotrimethylene Trinitramine (RDX) with Metal–Organic Framework IRMOF-1

ARTICLE *in* THE JOURNAL OF PHYSICAL CHEMISTRY C · FEBRUARY 2010

Impact Factor: 4.77 · DOI: 10.1021/jp905459h

6 AUTHORS, INCLUDING:

Khorgolkhuu Odbadrakh
Joint Institute for Computational Sciences,...
34 PUBLICATIONS **106** CITATIONS
SEE PROFILE

James P Lewis
West Virginia University
90 PUBLICATIONS **2,796** CITATIONS
SEE PROFILE

Tetyana Petrova
Jackson State University
11 PUBLICATIONS **114** CITATIONS
SEE PROFILE

Andrea Michalkova
45 PUBLICATIONS **662** CITATIONS
SEE PROFILE

Interactions of Cyclotrimethylene Trinitramine (RDX) with Metal−Organic Framework IRMOF-1

Khorgolkhuu Odbadrakh,*,† James P. Lewis,† Donald M. Nicholson,‡ Tetyana Petrova,§ Andrea Michalkova,§ and Jerzy Leszczynski§

Department of Physics and Astronomy, Box 6315, West Virginia University, Morgantown, West Virginia, 26506-6315, Computer Science and Mathematical Division, Oak Ridge National Laboratory, P. O. Box 2008, Oak Ridge, Tennessee 37831-6164, and Computational Center for Molecular Structure and Interactions, Department of Chemistry, Jackson State University, 1325 Lunch Street, Jackson, Mississippi 39217-0510

Received: June 10, 2009; Revised Manuscript Received: November 20, 2009

In this paper, we report on the interactions of 1,3,5-trinitro-s-triazine, or cyclotrimethylene trinitramine (RDX), a highly explosive (HE) molecule, with the metal−organic frameworks (MOF) called IRMOF-1. IRMOFs are predicted to act as preconcentrators for explosive molecules or other adsorbates because of their high porosity and selectivity through changeable organic linkers. We choose IRMOF-1 as a benchmark test case for further investigations of MOF−HE interactions. We use the density-functional-theory-based code FIREBALL to estimate physisorption energies for the RDX molecules both in the interior and on surfaces of IRMOF-1 cages. Our calculations show that the RDX molecules interact more strongly with the exterior IRMOF-1 surface than with the interior one, suggesting an important role of steric hindrance inside periodic IRMOF-1 cages. We extended our investigations to molecular-dynamics simulations at room temperature to see if any trapping configurations of RDX molecule result from the configurations at zero temperature.

I. Introduction

Metal−organic frameworks (MOFs) are a new class of nanoporous materials with promising physical and chemical properties for gas adsorption, storage, and separation.[1−3] MOFs have high internal surface areas (1000−5400 m^2/g), high porosity (2900 m/g), and tailorable pore size (Figure 1a); therefore, they have the potential of acting as selective absorbents for preconcentrator devices.[4] In MOFs, metal-oxide clusters are connected by organic linkers in three-dimensional crystalline structures with well-defined pores and cavities at the nanoscale, making their bulk volume accessible for relatively large molecules. The MOF cage size can be uniformly changed by using different organic linkers, resulting in different pore sizes and electrochemical properties of the crystalline structure, which in turn can enhance the selectivity of interactions with guest molecules.[5] Organic linkers in MOFs can be decorated with additional funcionality, increasing the possibility to make MOFs highly selective.[6] Applications of MOFs discussed in the literature include catalysts for storage of methane,[7] hydrogen,[8] and CO_2,[9] gas separation,[10] alkynes conversion,[11] and ammonia.[12]

In this research, we focused on the MOFs as preconcentrators[13] of explosive molecules, because of their potential application in selectively absorbing and concentrating trace amounts of commonly used explosives. The use of MOFs in explosive detection technology could potentially contribute to reduced cost for public security. The highly tailorable structure of MOFs may allow the design of selective absorption of certain explosive molecules, thus increasing efficiency while reducing time and cost of the detection process.[13] Commonly used preconcentrators, such as zeolites and carbons, require large amounts of the materials to be exposed to a target air environment for extended period of time. Because of their nonselective nature, preconcentrators also absorb nontarget substances that further complicate the detection process.[14] At this point, there are very few published reports on the interaction of MOFs with explosive molecules.[15] In this report, we present results of investigations on the interactions of cyclotrimethylene trinitramine (RDX) molecules with IRMOF-1 by using atomic -orbital-based DFT approach. We choose IRMOF-1 as a benchmark test case for further investigations of MOF−highly explosive (HE) interactions. The connector in IRMOF-1 is composed of Zn_4O tetrahedron extended by CO_2 groups on each of the tetragon's sides (Figure 1b), and the organic linkers for IRMOF-1 are benzene rings. IRMOF-1 is one of the extensively studied MOFs and known to have excellent selective absorbent for phosphonates, with concentration gains of over 5000 times for dimethyl methylphosphonate (DMMP) with sampling times of 4 s. By comparison, the Tenax TA has a preconcentration

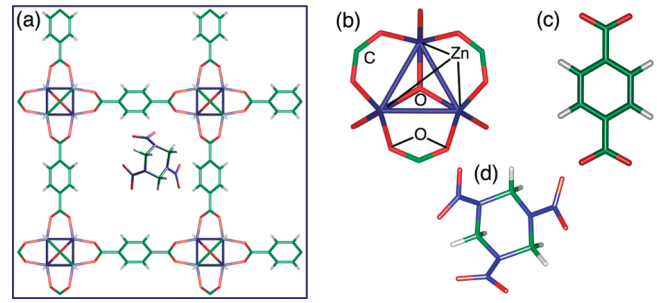

Figure 1. Geometric configurations of different IRMOF components: (a) IRMOF-1 cage with RDX in its bulk, (b) Zn_4O connector of IRMOF-1, (c) organic linker of IRMOF-1, and (d) RDX explosive molecule.

* Corresponding author. E-mail: od.odbadrakh@mail.wvu.edu.
† West Virginia University.
‡ Oak Ridge National Laboratory.
§ Jackson State University.
† Electronic address: james.lewis@mail.wvu.edu

10.1021/jp905459h
Published on Web 02/10/2010

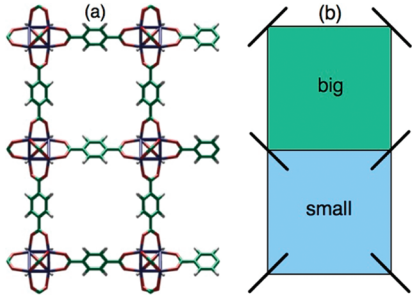

Figure 2. (a) Slab of IRMOF-1 terminated at C atoms for surface calculations and (b) schematic illustration of big and small cages in the IRMOF-1.

gain of only two-fold. The selective nature of IRMOF-1 is demonstrated with dodecane concentration gain of only five times.[14]

Interactions of guest molecules with the bulk IRMOF-1 should be viewed in two distinct classes due to two different accessible volumes within IRMOF-1; depending on the orientation of benzene rings, IRMOF-1 has either a big or a small cage in its crystalline structure. The schematic view of the big and small cages are shown in Figure 2b. It has been reported in recent studies[15] that the big and small cages inside the IRMOF-1, caused by orientation of the organic linkers, differ in their ability to trap RDX molecules.

RDX is a commonly used HE molecule (Figure 1c), found in many forms such as plastic explosives. Most of the previous investigations on the potential applications of MOFs focus on absorption or trapping of guest molecules inside MOF cages. We conducted this investigation with special emphasis on investigating interactions of RDX molecules with the IRMOF-1 surface as well as with the interior. The IRMOF-1 surface is the first interface guest molecules would encounter during the preconcentration process; thus, it is crucial to investigate the underlying physical and binding processes occurring on this surface. Also, IRMOF-1 is manufactured in nanoparticles form,[16] which implies the importance of the surface because of the large surface area per unit mass of nanopowders. The large-scale quantum simulations that we employed enable us to realistically model both bulk and surface interactions of IRMOF-1 with RDX; the unit cell contains over 300 atoms. We discuss our approaches and methodologies in Section II, followed by discussion of our results in Section III. In the end, we briefly summarize our findings in Section IV.

II. Methodology

We use FIREBALL,[17] a fully self-consistent, density-functional-theory (DFT)-based code to perform lattice-optimization, energy, electronic-structure, and molecular-dynamics (MD) calculations. The code uses atomic orbitals (fireball orbitals) to express atomic wave functions with finite cutoff lengths.[18] This cutoff results in a slight increase of the orbital energy (0.15 Ryd excitation) because of the finite size effect (Fermi compression). In general, the basis set must be chosen with chemically justified cutoff lengths for the eigenfunctions.[19] Double-numerical (excited states) orbitals have been added to provide additional degrees of freedom for atomic interactions. Each orbitals within these basis sets have been further refined by using confining potentials to adjust tails of the basis functions to an exponential form.[20] We use the Becke form of the exchange interactions[21] with a Lee−Yang−Parr correlation interactions[22] for all of the FIREBALL calculations presented here. Forces for each atom are determined by using a variation of the Hellmann−Feynman theorem.[23] The equations of motion are solved by using a Gear predictor−corrector algorithm, and the resulting kinetic energy is calculated, for which the velocities are quenched for a maximum kinetic energy defined by the temperature of the system. The process is repeated until a zero-force configuration is obtained.[24] In general, this is a first-principles-derived tight-binding-like methodology, and it is known to accurately calculate electronic structures of many complex systems.[25] Details of the methodology are extensively discussed elsewhere, and we refer readers to the literature.[18,29]

To optimize the MOF cage, we started energy minimization calculations at $T = 0$ K at different lattice constants a_0. For optimization, we chose a primitive unit cell consisting of 106 atoms and the principal lattice vector close to the experimental value. We then compared the resulting energies for each volume by using simple cubic fitting curve to obtain the equilibrium lattice constant a_0.

Surface interactions between the RDX molecule and the MOF are key to the adsorption and preconcentration processes. If the adsorption on a surface dominates the interactions, a design strategy for the proposed preconcentrator should be focused more on creating larger external surface areas by manufacturing smaller nanoparticles of MOFs rather than synthesizing larger particles. Therefore, we studied interactions of RDX on the MOF with special emphasis on surfaces. IRMOF-1 is terminated at CO_2 atoms along the (001) direction and subjected to surface relaxations (see Figure 2a). Three linker planes have been taken to satisfy mirror symmetry of the slab along the center plane, and super-cell parameters have been chosen so that the slab has a large vacuum at its top and bottom; this simulation super cell consists of 308 atoms.

For the combined IRMOF-1/RDX system, we performed optimization of the structure at $T = 0$ K to calculate the interaction energies or activation barriers if any. We chose the most stable AAE conformation of RDX molecule as an initial geometry for all our simulations. The RDX molecule is originally placed at binding sites suggested by Michalkova et al.[27] with slightly shorter bond lengths. This initial placement reduces transient time for the RDX molecule to settle in its most probable final configuration. The energetics of the combined system is the key information that describes the interactions between the IRMOF-1 cage and the RDX molecule. The interaction energy is given by

$$\Delta E = E_{(\mathrm{MOF+RDX})} - (E_{\mathrm{MOF}} + E_{\mathrm{RDX}}) \qquad (1)$$

where $E_{(\mathrm{MOF+RDX})}$, E_{MOF}, and E_{RDX} are the total energies of MOF−RDX compound system, MOF cage, and adsorbate (the isolated RDX molecule), respectively.

We further extended our investigation by MD simulations to explore how the physisorption configurations at $T = 0$ K are affected at finite temperature. Primary goal of the MD simulations in this work is to obtain, starting from the optimized configurations at $T = 0$ K, informed guess on the nature of trapping configurations of RDX molecule by IRMOF-1 at room temperature. Detailed studies on a similar but much larger system have been performed by our collaborators by using a grand-canonical MD method. Therefore, we refer readers to their work.[15] For the MD simulations, we used a number-volume-temperature (NVT) ensemble with an explicit-velocity Verlet integrator, which uses the factorized Liouville operator to calculate time evolution of the atomic positions. The Hamiltonian is modified to a nonconservative system by adding a series of damped oscillator terms to the potential energy. Then, a

TABLE 1: Atomic Bond Lengths of IRMOF-1 Cage Obtained by Using FIREBALL Atomic Orbitals Compared to Values Obtained through Quantum-Chemical Calculations[37] and Experiments[38,a]

method	Zn−O_1	Zn−O_2	C−O_2	C−C
B3LYP/I	1.969	1.972	1.272	1.495
B3LYP/II	1.953	1.948	1.271	1.493
B3LYP/III	1.975	1.973	1.264	1.494
Exp-1	1.933−1.945	1.937−1.969	1.244−1.267	1.488−1.501
Exp-2	1.936−1.950	1.930−1.950	1.234−1.270	
FIREBALL	1.956	1.981	1.313	1.515

[a] Lengths are in angstroms.

Nosé−Hoover chain thermostat was used to control temperature,[28,29] allowing the system to cool/heat if the instantaneous kinetic energy is higher/lower than kBT, where T is the desired temperature. When choosing the optimized IRMOF-1/RDX structures at $T = 0$ K as starting configurations, we first increased the temperature to 300 K and then ran the MD simulations for 7 ps while tracking the position of the center of mass of the RDX molecule.

The physisorption configurations obtained at $T = 0$ K are not expected to remain at room temperature, and combination of long-range interactions such as steric hindrance, electrostatic, and van der Waals (vdW) forces are expected to be main contributors. As a result, the trapping mechanism for the HE molecules at room temperature is of different nature than physisorption at $T = 0$ K and could be better described as molecular sieving or quantum sieving. We added empirical vdW terms with a cutoff radius of 9. 0 Å and parameters C_6, alpha (polarizability), and R_0 for each atomic species for MD simulations at room temperature. As in schemes provided in refs 30 and 31, the dispersive energy is described by damped interatomic potentials of the form (C_6R^{-6}). Although it is known that the empirical vdW approach has its limitations, it has been successfully used in combination with DFT on many systems.[31−35] We tested the empirical vdW terms by calculations at 0 K for IRMOF-1/RDX system, for which contributions to interaction energies averaged at 2%, suggesting that vdW forces alone are not the dominant player for this system. Therefore, we did not include the empirical vdW terms for calculations at 0 K.

III. Results and Discussions

a. Lattice Optimizations at $T = 0$ K. We have probed several different basis sets for optimizing the IRMOF-1 lattice, and the best performing set includes double numerical basis set for C and O atoms and a minimal basis set for H and N atoms. We also include a semicore 3d orbital for Zn. This basis set produces a lattice constant $a_0 = 26.118$ Å, which is within 1.0% of an experimental value $a_0 = 25.885$ Å,[5] as well as values obtained by using other DFT-based computational tools, $a_0 = 25.888$ Å[36] and $a_0 = 25.614$ Å.[13] Individual bond lengths are slightly longer than accepted experimental values but comparable with values obtained by quantum-chemistry calculations (Table 1). However, note that the quantum-chemistry calculations are cluster calculations. Expanding the basis set with d orbitals for C or O atoms did not improve the lattice optimization. Overall, our best performing basis set predicts the lattice constant and bond lengths accurately for the purpose of performing MD simulations and electronic-structure calculations. In our investigations of the surface interactions of RDX, we optimized the surface of the IRMOF-1 by using three layers of linker planes terminated at the CO_2 group (Figure 2a). Predictably, there are no surface reconstructions due to this termination, and the bond lengths near the surface changed only slightly; therefore, the IRMOF-1 surface has a well-defined structure close to its bulk parameters.

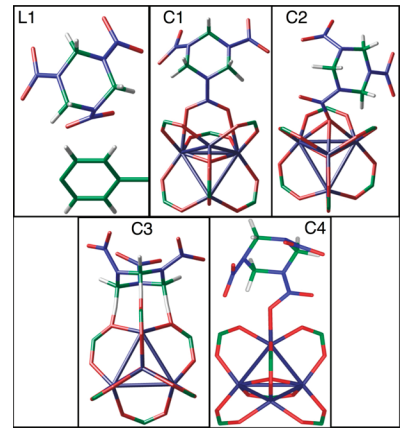

Figure 3. Binding configurations for RDX: L1 on a linker and C1, C2, C3, and C4 are on a connector. The configurations C3 and C4 are in the bigger cage.

b. RDX in the IRMOF-1 Cage at $T = 0$ K. We investigated six binding configurations (all shown in Figure 3) of the RDX molecule with IRMOF-1. For simplicity, we name and define these different binding configurations as follows:

L1, hydrogen bonding of a NO_2 group of the RDX to two CH groups on the linker;

C1, bonding of both O atoms of a NO_2 group of RDX to two Zn atoms of a connector;

C2, bonding of a single O atom of the NO_2 group of RDX to three Zn atoms of a connector;

C3, bonding of three CH groups of the RDX to three O atoms of a connector;

C4, bonding of RDX to one of the Zn atoms in the IRMOF-1 connector through its O atom of NO_2 group;

We first optimized these initial binding configurations through energy minimization at $T = 0$ K and then performed single-step energy calculations for the isolated RDX molecule and MOF cage separately in order to calculate the binding energies. We set the bond lengths between the binding atoms of IRMOF-1 and RDX to 1.75 Å initially on the basis of quantum-chemistry calculations, and then, we relaxed these structures. Effects of MOF frame flexibility on adsorption of guest molecules were previously studied and to their role in accessing the internal porous areas of the cage by the guest molecules was pointed out.[39−41] In this work, however, we exclusively focus our studies on finding the energetically feasible binding interactions of RDX molecules with IRMOF-1 structure units; therefore, we limit our modeling to fixed IRMOF-1 atoms and freely moving RDX atoms. We allow IRMOF-1 charges to adjust self-consistently. The interaction energies for the configurations L1, C1, C2, C3, and C4 are given in Table 2.

Initially, we consider calculations using FIREBALL of the above-mentioned configurations in a cluster approach and compare results with standard quantum-chemistry calculations using GAUSSIAN (a 6-311G** basis with B3LYP). As shown in Table 2, we were able to simulate configurations L1, C2, and C3 both in cluster and periodic configurations of IRMOF-1, whereas configurations C1 and C4 were not available from the quantum-chemisty simulations. Also, our simulations failed to obtain metastable states for configurations C5 and C6, which are denoted by an asteric in the table. We find that our optimizations reproduce the geometry and bond lengths in these cluster structures to within 0.5% of the values determined by

TABLE 2: Interaction Energies for RDX Binding Configurations Inside and on the Surface of The IRMOF-1 Cage[a]

	L1	C1	C2	C3	C4	C5*	C6*
cluster I	−0.45		−20.5	−11.23		−13.00	−3.05
cluster II	−5.60		−4.90	−2.40		−4.40	−9.8
interior (periodic)	−37.02	+1.61	+1.00	+17.86	+10.00		
surface (periodic)	−31.57	−224.19	−117.74	−81.79	+41.70		

[a] The interaction energies are given in units of kcal/mol. Cluster I denotes cluster energies calculated by using FIREBALL, and cluster II denotes results obtained by using GAUSSIAN.[27]

the quantum-chemistry calculations. Additionally, energies of the RDX molecule to the IRMOF-1 fragments show binding in all of the cluster-calculation case with the cluster-I cases tending toward overbinding compared to cluster-II cases. We believe that differences in the binding energies presented solely result from differences in basis sets and exchange correlations (BLYP vs B3LYP) in our DFT calculations.

In contrast, the interactions in the interior of the IRMOF-1 is mostly nonbinding, except in the case of L1 configuration. The difference in binding energies compared to the cluster calculation most likely results from steric constraints that the RDX molecule encounters while inside the IRMOF-1 structure. For the periodic system, the hydrogen−oxygen bond lengths in the periodic system converge to ∼1.85 Å (whereas the value provided by cluster calculations is ∼2.45 Å).[42] Our results show that the linkers (e.g., such as in the L1 configuration) are preferred binding sites for RDX inside the IRMOF-1 cage, whereas the connectors do not provide interior binding sites for the RDX molecule. Interactions of RDX with the bulk IRMOF-1 can also be viewed in two distinct classes due to two different accessible volumes within IRMOF-1; depending on the orientation of benzene rings, IRMOF-1 has either a big or asmall cage in its crystalline structure (Figure 2b). Configurations C1 and C2 are in the bigger cage, and configurations C3 and C4 are in the smaller cage of the IRMOF-1. All four configurations show nonbinding inside the IRMOF-1 structure.

c. RDX on the IRMOF-1 Surface at $T = 0$ K. Interestingly, the surface-optimization results offer binding results contrary to the values provided by interior calculations because steric constraints are removed. Additionally, our results exhibit very strong binding compared to the cluster calculations. We attribute these differences primarily to the fact that full periodicity of the extended IRMOF-1 structure is considered in these calculations with full long-range coulomb interactions, whereas the cluster calculations are performed only on IRMOF-1 fragments. Our results indicate that, particularly for these porous structures, full periodicity definitively will yield results which are more physical because long-range forces must be considered for accuracy. This statement is particularly more true when more polar linkers are considered in order to build very selective MOFs for RDX absorption purposes.

d. RDX/IRMOF-1 Interaction at Room Temperature. Strong interactions of RDX molecule with the IRMOF-1 cage at room temperature is crucial for any practical use of IRMOF-1 as explosive preconcentrator. The goal of MD simulations in this work is to probe possibilities of physisorptions of the RDX with IRMOF-1 at room temperature. IRMOF-1 is known to be stable well above room temperature and still efficient in absorbing a range of gas molecules.[6] We performed constant-temperature MD simulations at $T = 300$ K for each of the binding configurations found at $T = 0$ K and observed trajectories of RDX molecules while the IRMOF-1 atoms are fixed; the simulations ran for 7 ps. As mentioned in Section II, we chose AAE as the initial conformation for RDX molecule for all our simulations, and it should be noted that we observed no change of conformation during the MD simulation. In general, the RDX molecules dissociate from their binding sites at 300 K and migrate toward the center of the cage, which is a more energetically favorable location because steric hindrances are minimized.

As a result of these simulations, we find two new configurations shown in Figures 4 and 5. We have found only one configuration inside the cage, for which the RDX molecule resided 50% of the 7 ps MD run (Figure 4, bottom) and kept its orientation with respect to the IRMOF cage (Figure 4, top). Energy calculations for this configuration result in a binding

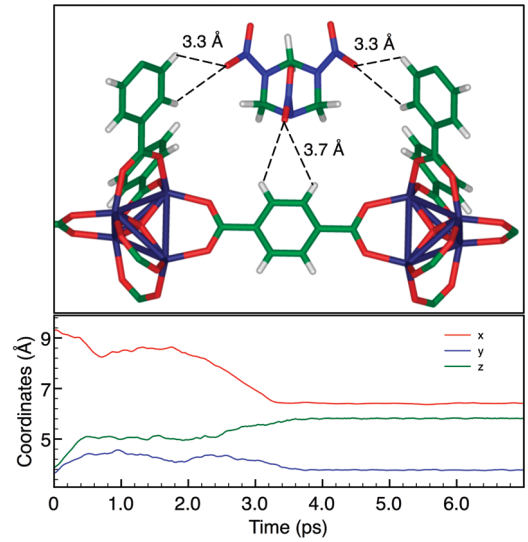

Figure 4. Stable binding configuration of RDX inside IRMOF-1 cage at $T = 300$ K (top) and coordinates of RDX center of mass for 7 ps MD run (bottom). The initial binding configuration is C4.

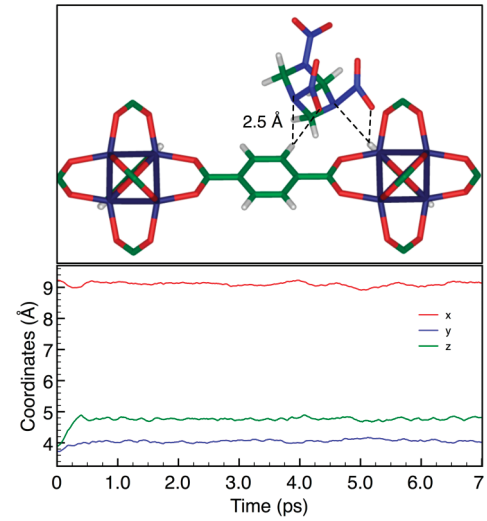

Figure 5. Stable binding configuration of RDX on IRMOF-1 surface at $T = 300$ K (top) and coordinates of RDX center of mass for 7 ps MD run (bottom). The initial binding configuration is C4.

energy of −110.65 kcal/mol, which makes it more energetically favorable than the nonbinding configurations found at $T = 0$ K. In this configuration, the RDX molecule is bound to three linkers in the small cage of the IRMOF-1 through O—H bonds, which are 3.3−3.7 Å on average. MD simulations at $T = 300$ K on the IRMOF-1 surface also result in the dissociation of the binding configurations found at $T = 0$ K, and the RDX molecule migrates to a different binding site. For example, given C4 configuration on the surface as initial condition, the RDX molecule moves, changes its orientation with respect to the IRMOF-1 (Figure 5, top), and finds itself in a new configuration in which it spends more than 90% of the 7 ps MD simulation (Figure 5, bottom). The binding energy of the RDX molecule with the IRMOF-1 surface in this configuration is −240.36 kcal/mol. Unlike the $T = 300$ K simulations starting from the C4 configuration, those that were started from configurations L1, C1, C2, and C3 (both in the bulk and on the surface) migrated away from the initial positions and continued to migrate over the surface during the 7 ps simulation.

IV. Summary

We investigated physisorption of RDX molecules in interior and on the surface of IRMOF-1. The goal of this study was to explore feasibility of using IRMOF-1 as an explosive preconcentrator. The main findings of this paper can be summarized as follows.

Steric hindrance plays an important role in the RDX-IRMOF-1 interactions. The same binding sites of RDX in interior and on the surface of IRMOF-1 have very different interaction energies. As a result, connectors in the interior of the IRMOF-1 periodic cage are not binding sites for RDX molecules, whereas linkers are the binding sites for the molecule. This may well be true for different variants of the MOFs because the topology of connectors and linkers remain basically the same. The IRMOF-1 surface is far more absorptive to the RDX molecule than its interior. In contrast to the bulk, the connectors on the surface are strong binding sites for the RDX molecule. Although the large surface area of IRMOF-1 makes more binding sites available, there are about 10^5 more internal binding sites in the bulk. Also, increasing the surface area by using small nanoparticles may potentially affect the overall efficiency of IRMOF-1 as selective preconcentrator of RDX molecules.

Within accuracy of our calculations, physisorption of RDX to IRMOF-1 is susceptible to temperature, both in the interior and the exterior of the cage. Our simulations at $T = 300$ K suggest at least one trapping configuration for RDX molecule inside IRMOF-1 cage, in which the RDX molecule is bound to three surrounding linkers of the smaller cage through hydrogen bonds. This indicates that long-range interactions become dominant factors at room temperature, giving rise to molecular sieving as the trapping mechanisms of the RDX molecules by IRMOF-8. To fully explore the use of IRMOF-1 as explosive preconcentrator for RDX molecule, MD studies of the system at room temperature must be further extended, including comparative investigations with experiments and computational studies of other porous materials.

Acknowledgment. We thank Dr. David Keffer for insightful discussions. We gratefully acknowledge the financial support of National Science Foundation (NSF) under Grant CMMI-0730207. Work at ORNL was performed under the auspices of the Division of Materials Science and Engineering, Office of Basic Energy Science of the US Department of Energy. Also, we thank Pittsburgh Supercomputing Center and WVNano for computing facilities.

References and Notes

(1) Yaghi, O.; Li, G.; Li, H. *Nature* **1995**, *378*, 703–706.
(2) Chae, H.; Siberio-Perez, D.; Kim, J.; Go, Y.; Eddaoudi, M.; Matzger, A.; O'Keeffe, M.; Yaghi, O. *Nature* **2004**, *427*, 523–527.
(3) Rowsell, J.; Yaghi, O. *Angew. Chem., Int. Ed.* **2005**, *44*, 4670–4679.
(4) Yaghi, O. M.; O'Keeffe, M.; Ockwig, N. W.; Chae, H. K.; Eddaoudi, M.; Kim, J. *Nature* **2003**, *423*, 705–714.
(5) Li, H.; Eddaoudi, M.; O'Keeffe, M.; Yaghi, O. *Nature* **1999**, *402*, 276–279.
(6) Rowsell, J.; Spencer, E.; Eckert, J.; Howard, J.; Yaghi, O. *Science* **2005**, *309*, 1350–1354.
(7) Eddaoudi, M.; Kim, J.; Rosi, N.; Vodak, D.; Wachter, J.; O'Keeffe, M.; Yaghi, O. *Science* **2002**, *295*, 469–472.
(8) Rosi, N.; Eckert, J.; Eddaoudi, M.; Vodak, D.; Kim, J.; O'Keeffe, M.; Yaghi, O. *Science* **2003**, *300*, 1127–1129.
(9) Millward, A.; Yaghi, O. *J. Am. Chem. Soc.* **2005**, *127*, 17998–17999.
(10) Mueller, U.; Schubert, M.; Teich, F.; Puetter, H.; Schierle-Arndt, K.; Pastre, J. Metal-organic frameworks -prospective industrial applications. *J. Mater. Chem.* **2006**.
(11) Chen, B.; Ockwig, N.; Millward, A.; Contreras, D.; Yaghi, O. *Angew. Chem., Int. Ed.* **2005**, *44*, 4745–4749.
(12) Sudik, A.; Millward, A.; Ockwig, N.; Cote, A.; Kim, J.; Yaghi, O. *J. Am. Chem. Soc.* **2005**, *127*, 7110–7118.
(13) Fuentes-Cabrera, M.; Nicholson, D.; Sumpter, B.; Widom, M. *J. Chem. Phys.* **2005**, 123.
(14) Ni, Z.; Jerrell, J. P.; Cadwallader, K. R.; Masel, R. I. *Anal. Chem.* **2007**, *79*, 1290–1293.
(15) Xiong, R.; Fern, J. T.; Keffer, D. J.; Fuentes-Cabrera, M.; Nicholson, D. M. *Mol. Simul.* **2009**, *35*, 910–919.
(16) Ni, Z.; Masel, R. I. *J. Am. Chem. Soc.* **2006**, *128*, 12394–12395.
(17) Lewis, J.; Glaesemann, K.; Voth, G.; Fritsch, J.; Demkov, A.; Ortega, J.; Sankey, O. *Phys. Rev. B* **2001**, *64*, 195103.
(18) Sankey, O. F.; Niklewski, D. J. *Phys. Rev. B* **1989**, *40*, 3979–3995.
(19) Ortega, J.; Lewis, J. P.; Sankey, O. F. *Phys. Rev. B* **1994**, *50*, 10516.
(20) Jelinek, P.; Wang, H.; Lewis, J. P.; Sankey, O. F.; Ortega, J. *Phys. Rev. B: Condens. Matter Mater. Phys.* **2005**, *71*, 235101.
(21) Becke, A. D. *Phys. Rev. A.* **1988**, *38*, 3098.
(22) Lee, C.; Wang, W.; Parr, R. G. *Phys. Rev. B.* **1988**, *37*, 785.
(23) Silvi, B. *THEOCHEM* **1991**, *72*, 129–145.
(24) Demkov, A.; Ortega, J.; Sankey, O.; Grumbach, M. *Phys. Rev. B* **1995**, *52*, 1618–1630.
(25) Liu, F.; Garofalini, S.; Kingsmith, R.; Vanderbilt, D. *Phys. Rev. Lett.* **1993**, *70*, 2750–2753.
(26) Sankey, O.; Demkov, A.; Windl, W.; Fritsch, J.; Lewis, J.; Fuentes-Cabrera, M. The application of approximate density functionals to complex systems. *Int. J. Quantum Chem.* **1998**.
(27) Leszczynski, J.; Petrova, T.; Michalkova, A. Theoretical Study of RDX and TATP Interactions with MOF-5. In Proceedings of the Physical Science and Technology Conference, 2008.
(28) Nose, S. *J. Chem. Phys.* **1984**, *81*, 511–519.
(29) Hoover, W. *Phys. Rev. A* **1989**, *40*, 2814–2815.
(30) Grimme, S. *J. Comput. Chem.* **2004**, *25*, 1463–1473.
(31) Elstner, M.; Hobza, P.; Frauenheim, T.; Suhai, S.; Kaxiras, E. *J. Chem. Phys.* **2001**, *114*, 5149–5155.
(32) Wu, Q.; Yang, W. *J. Chem. Phys.* **2002**, *116*, 515–524.
(33) Dong, H.; Hua, S.; Li, S. *J. Phys. Chem. A* **2009**, *113*, 1335–1342.
(34) Williams, R. W.; Malhotra, D. *Chem. Phys.* **2006**, *327*, 54–62.
(35) Du, A.; Smith, S. *Nanotechnology* **2005**, *16*, 2118–2123.
(36) Mattesini, M.; Soler, J.; Yndurain, F. *Phys. Rev. B* **2006**, 73.
(37) Tafipolsky, M.; Amirjalayer, S.; Schmid, R. *J. Comput. Chem.* **2007**, *28*, 1169–1176.
(38) Clegg, W.; Harbron, D.; Homan, C.; Hunt, P.; Little, I.; Straughan, B. *Inorg. Chim. Acta* **1991**, *186*, 51–60.
(39) Forester, T.; Smith, W. *J. Chem. Soc. Faraday Trans.* **1997**, *93*, 3249–3257.
(40) Jakobtorweihen, S.; Verbeek, M.; Lowe, C.; Keil, F.; Smit, B. *Phys. Rev. Lett.* **2005**, 95.
(41) Fletcher, A.; Thomas, K.; Rosseinsky, M. *J. Solid State Chem.* **2005**, *178*, 2491–2510.
(42) Michalkova, A.; Petrova, T.; Leszczynski, J.; Keffer, D.; Nicholson, D. M.; Fuentas-Cabrera, M.; Lewis, J. P. In Proceedings of the Physical Science and Technology Conference, 2009.

JP905459H